Journal of Engineering Mathematics **28**: 73–91, 1994.

On global and internal dynamics of spots: a theoretical approach

F.T. SMITH, B.T. DODIA and R.G.A. BOWLES

Department of Mathematics, University College London, Gower Street, London WC1E 6BT, United Kingdom

Received 7 January 1993; accepted in revised form 17 August 1993

Abstract. Nonlinear effects on the free evolution of three-dimensional disturbances are discussed, these disturbances having a spot-like character sufficiently far downstream of the initial disturbance. The inviscid initial-value formulation taken involving the three-dimensional unsteady Euler equations offers hope of considerable analytical progress on the nonlinear side, as well as being suggested by some of the experimental evidence on turbulent spots and by engineering modelling and previous related theory. The large-time large-distance behaviour is associated with the two major length scales, proportional to $(\text{time})^{1/2}$ and to (time), in the evolving spot; within the former scale the Euler flow exhibits a three-dimensional triple-deck-like structure; within the latter scale, in contrast, there are additional time-independent scales in operation. As the typical disturbance amplitude increases, nonlinear effects first enter the reckoning in edge layers near the spot's wing-tips. The nonlinearity is mostly due to interplay between the fluctuations present and the three-dimensional mean-flow correction which varies relatively slowly. The resulting amplitude interaction points to a subsequent flooding of nonlinear effects into the middle of the spot. There it is suggested that the fluctuation/mean-flow interaction becomes strongly nonlinear, substantially altering the mean properties in particular. A new global viscous-inviscid interaction between the short and long scales present, involving Reynolds stresses, is also identified. The additional significance of viscous sublayer bursts is also noted, along with comments on links with experiments and direct numerical simulations, on channel flows and jets, and on further research.

1. Introduction

The development of the three-dimensional 'spot' or travelling disturbance from an initial localized disturbance in an otherwise laminar boundary layer involves mainly downstream travel, some amplitude growth and spatial spreading of the spot. Three basic types of spot may be identified, namely laminar, transitional and turbulent, depending on the amplitude and spectra of the initial disturbance. All three are of much interest in terms of the fundamental fluid dynamics involved and the applications.

Many experimental studies have been made on various aspects of turbulent spots, with fascinating and somewhat varied results, for example on the main arrowhead-shaped part of the spot, on its tail, on the notional speed of the spot, on its spreading rate, and so on. See Emmons [1], Katz et al. [2], Glezer et al. [3], Riley and Gad-el-Hak [4], Perry et al. [5], Walker [6], Falco [7], C.R. Smith et al. [8], Gad-el-Hak et al. [9], Bandyopadhyay [10], Lighthill [11], Schlichting [12], Chambers and Thomas [13], Wygnanski et al. [14], Schubauer and Klebanoff [15], Head and Bandyopadhyay [16], Johansson et al. [17], Henningson and Alfredson [18], Robinson [19], and other papers in this issue of *J. Eng. Maths*. Outstanding features found experimentally include the following. (a) Much of the dynamics in a spot resembles closely that in a fully turbulent boundary layer. (b) A turbulent spot develops fast, typically from localized disturbances with large initial amplitude. (c) The growth and spreading of a fully turbulent spot probably take place in a domino-like manner, possibly associated with the successive production of hairpin vortices in the flow near the solid surface. (d) The spanwise growth of the spot greatly exceeds the growth normal to the surface. (e) The front and the spanwise side edges, or wing-tips, of the spot are notably

sharp, with interaction between the spot and trailing wave packets especially near the wing-tips. Several other experimental features of interest are also described in the above papers.

Again, interesting computations have been performed on transitional/turbulent spots, mostly for channel flows and more recently for boundary layers. Most are confined to simulations with spatially periodic boundary conditions but, for a large period, they seem to reproduce fairly well some of the major experimental findings. Examples are in Leonard [20], Bullister and Orszag [21], Henningson et al. [22], Henningson and Kim [23], Lundbladh and Johansson [24], Fasel [25], Fasel and Konzelmann [26], and other papers in this issue. Much extra physical insight and understanding have still to be provided, nevertheless. Systematic tracking of the effects of increasing amplitude for instance largely remains to be done, both experimentally and computationally, apart perhaps from Henningson et al. [27] and Cohen et al. [28] upon which comments are made near the end of this section.

Until recently little or no systematic theory/analysis had been done either, as far as we know, especially on the scales and flow structures necessary for a clear physical understanding of the spots' behaviour. A strongly nonlinear theory is desirable but except for the research below there appears to be no substantial effort in that direction, specifically for spot evolution, i.e. the initial-value problem. Our prime aim here combined with the related works (Doorly and Smith [29], Smith [30, 31], see also Gaster [32]), as far as possible, is to review and develop recent nonlinear theory and in particular address the experimental findings (a)–(e) above. Much of these findings can be described by the theory, taken in conjunction with the study of Smith et al. [33], even though many complex phenomena arise during spot evolution in practice, there is significant dependence on the particular experimental configurations and conditions used, and there are many nonlinear aspects still to be explained or explored.

The Euler stage of Smith et al. [33], Smith and Burggraf [34] appears to be the closest, of any rational theory for high Reynolds numbers (Re), to describing boundary-layer turbulence in a systematic fashion. That view is supported in the two last-named papers and also by the more empirical modelling of Walker [6]; see also C.R. Smith et al. [8], Hoyle et al. [34], Peridier et al. [35, 36]. The local flow within the boundary layer is then controlled predominantly by the three-dimensional [3D] unsteady nonlinear Euler equations, according to the above description/model, apart from interludes, however brief, when eruption of the otherwise thin viscous sublayer occurs near the surface and injects a substantial burst of localized vorticity into the Euler flow (see also §7 below). This Euler stage corresponds to nonlinear disturbance wavenumbers α, β, frequencies ω, propagation speeds c and amplitudes (e.g. pressure p', velocity $\underline{u}'$) all of $O(1)$, based on the boundary-layer thickness and local freestream speed, thus representing a wider range than conventional linear-type Tollmien–Schlichting disturbances which have α, β, ω, c, $|p'|$, $|\underline{u}'|$ all smaller by an order of magnitude. In consequence, it seems not unreasonable to tackle the spot-evolution problem theoretically first by means of the same Euler-stage nonlinear approach, but as a nonlinear 3D initial-value problem for a localized input disturbance (rather than a fixed-frequency problem, for example). That indeed is the concern of much of this article.

In §2 below the governing equations are presented, with attention being drawn to the "trailing-edge" region existing between the two main zones with length scales of order $(\text{time})^{1/2}$ and (time) downstream, in nondimensional terms. It is something of a surprise to find that the solution of the 3D Euler equations acquires a 3D triple-deck form, within the $(\text{time})^{1/2}$ scale just mentioned. The article then moves on, in §3, to nonlinear effects acting

near the wing-tips or side edges of a spot, since the earlier linear theory of Doorly and Smith [29] suggests that is where nonlinearity may appear first naturally as the typical input amplitude is increased or as the spot progresses further downstream. This also has possible connections with the experimental finding (e) above. The linear theory just mentioned, in which the initial-value problem can be solved in exact form for some contexts, shows the emergence of a number of distinct zones downstream at comparatively large times, the two main length scales induced being proportional to the scaled time and to its square root. The maximum amplitude, however, is produced in a relatively thin region near the wing-tip of such a linear spot. That property, along with the near-neutrality of the linear-spot behaviour at large times and distances, motivates the study of nonlinear wing-tip effects first. Moreover, these effects are found to lead on subsequently to other cases, corresponding to further increases in the typical amplitudes, where nonlinearity gradually floods into the middle portion of the spot [§§4, 5].

The major responses in §§3, 4 arise from interaction between the dominant fluctuations, or fast waves, and the 3D mean-flow correction, with the wall-layer and critical-layer influences diminished in relative terms. The resulting nonlinear amplitude equations in turn lead on to certain significant percussions regarding strongly nonlinear effects at substantially increased amplitudes, where interesting scales emerge which seem to be physically sensible, for the middle of the nonlinear spot (§5). This study and the related works also suggest possible new experiments of interest, and direct computations, regarding the effects of increased input amplitudes on spot evolution.

Sections 6–8 then deal respectively with the O(time) zone further downstream, with viscous effects particularly from the assumed thin wall sublayers, and with further comments including experimental comparisons and links and the applications to channel flows and wall jets.

The current work tends to split the spot dynamics into two categories, global (mainly inviscid) and internal (viscous-inviscid) properties, and to concentrate on the former throughout §§2–6. Nevertheless, a new long/short-scale global interaction is identified in §6, linking the 3D viscous boundary-layer equations and unsteady Euler equations via Reynolds-stress forces, sufficiently far downstream. Internal properties, flow structures and their interactions with the more global dynamics are summarized briefly in §7 and are addressed in more detail in the recent literature cited there. Although, as a starting point, the viscous sublayer and its eruptions are neglected at first, these eruptions and the ensuing local vortex formations (§7) can become important in practice, and they are the subject of recent theoretical and/or computational studies by Smith [37], Hoyle et al. [34], Peridier et al. [35, 36], as reviewed by Smith [38], Walker [6], C.R. Smith et al. [8] for example. Not least, they introduce shorter length and time scales, and hence even higher frequency and wavenumber content, and they almost certainly play a key part in the domino process mentioned earlier.

The global Reynolds number Re, based on the airfoil chord and free-stream in the aerodynamic context for example, is assumed large, and we address here the 3D nonlinear incompressible régime. The work is aimed eventually at relatively high-amplitude nonlinear responses, as opposed to gradual transition following linear instability for instance (see also comments in Doorly and Smith [29] and related papers). The latter transition for spots is considered in Cohen et al.'s [28] interesting, mainly experimental, study, i.e. with input spectrum corresponding essentially to longer, Tollmien–Schlichting, length and time scales, lower amplitudes and relatively slow propagation (until breakdown occurs later on), in

contrast with the present wider spectrum of faster, Euler, scales, higher amplitudes and faster propagation, equivalent to a nonlinear by-pass mechanism. The extension to compressible boundary layers started by Doorly and Smith [29] needs following through and there may be impact also in several other areas, including ship wakes. Many issues and aspects are left unresolved, of necessity, and research on some of these is in progress. Again, we should emphasize that we do not claim uniqueness in the nonlinear spot behaviour for relatively large times and distances. Alternative effects might include resonant or other interactions and stronger unsteady or nonlinear critical-layer effects. The major physical effects investigated here however are through nonlinear interactions between the fluctuations present and the mean flow.

2. The nonlinear governing equations, and the spot trailing-edge

The main context concerns the Euler stage for large fully nonlinear disturbances (Smith and Burggraf [34]; Smith et al. [33]) where the unsteady nonlinear 3D incompressible Euler equations apply,

$$u_x + v_y + w_z = 0\,, \tag{2.1a}$$

$$u_t + uu_x + vu_y + wu_z = -p_x\,, \tag{2.1b}$$

$$v_t + uv_x + vv_y + wv_z = -p_y\,, \tag{2.1c}$$

$$w_t + uw_x + vw_y + ww_z = -p_z\,, \tag{2.1d}$$

throughout the boundary layer, at large global Reynolds number Re. Here the non-dimensional velocity components u, v, w and the corresponding x, y, z cartesian coordinates (streamwise, normal and spanwise, respectively, with an origin shift) are scaled with respect to the local free-stream speed and the typical boundary-layer thickness $O(\mathrm{Re}^{-1/2})$, in turn, and similarly for the $O(\mathrm{Re}^{-1/2})$ timescale t and the $O(1)$ pressure scale p. The main boundary conditions are

$$(u, v, w, p) \to \begin{cases} (u_e, 0, w_e, 0) & \text{as } y \to \infty\,, \quad (2.2a) \\ (u_B(y), 0, w_B(y), 0) & \text{as } x^2 + z^2 \to \infty\,, \quad (2.2b) \end{cases}$$

$$v = 0 \text{ at } y = 0\,, \tag{2.2c}$$

where the conditions (2.2a, b) are to match with the free stream outside the boundary layer and with the undisturbed boundary-layer profile $u_B(y)$ holding sufficiently far from the initial disturbance, and (2.2c) is the tangential-flow constraint at the solid surface. For the present, $u_e \equiv 1$, $w_e = w_B(y) \equiv 0$. The profile $u_B(y)$ is supposed here to be monotonic, inflexion-free, and $u_B(\infty) = 1$, $u_B'(0) = \lambda_B > 0$. An example is the Blasius profile. The initial disturbance itself is fully nonlinear in general, so that

$$(u, v, w, p) \text{ is prescribed (for all } x, y, z) \text{ at } t = 0\,, \tag{2.3}$$

consistent with (2.1a–d). The problem (2.1a)–(2.3) is a computational one usually.

The current work addresses the issue of the possible solution properties of the nonlinear

initial-value problem above at large times, and especially far downstream of the initial-disturbance position, given guidance from the linearized analysis of Doorly and Smith [29]. At large times t two major length scales arise in the plan-view (xz plane), one very far downstream at distances $O(t)$ and the other less far downstream, at distances $O(t^{1/2})$. These two scales also occur in the Doorly and Smith work. Below we are concerned primarily with the $O(t^{1/2})$ length scale, since certain significant features are found to arise first there, even though this is the zone that trails the majority (the $O(t)$ zone, see §6) of the spot. See Fig. 1. An order-of-magnitude argument suggests the perhaps surprising feature that, in the $O(t^{1/2})$ zone, the large-time solution of the unsteady Euler problem (2.1a)–(2.3) takes on a three-layer form, analogous with the triple-deck structure. The 'lowest' layer has y being small, with

$$[u, v, w, p] \sim [t^{-1/2}U, t^{-3/2}V, t^{-1/2}W, t^{-1}P], \quad y = t^{-1/2}Y, \tag{2.4a}$$

whereas in the 'middle' layer

$$[u, v, w, p] \sim [u_B(y) + t^{-1/2}Au_B', -t^{-1}A_X u_B(y), O(t^{-1}), t^{-1}P], \qquad y = O(1), \tag{2.4b}$$

and in the 'uppermost' layer in the outer reaches of the boundary layer

$$[u, v, w, p] \sim [1 + t^{-1}\bar{u}_1, t^{-1}\bar{v}_1, t^{-1}\bar{w}_1, t^{-1}\bar{p}], \qquad y = t^{1/2}\bar{y}. \tag{2.4c}$$

Here the unknown surface pressure $P(X, Z)$ and negative displacement $A(X, Z)$ depend only on the scaled coordinates X, Z defined by

$$(x, z) = t^{1/2}(X, Z) \tag{2.5}$$

in the present zone. The main resulting governing equations are those for the lowest layer, namely

$$U_X + V_Y + W_Z = 0, \tag{2.6a}$$

$$-\tfrac{1}{2}U + (U - \tfrac{1}{2}X)U_X + (V + \tfrac{1}{2}Y)U_Y + (W - \tfrac{1}{2}Z)U_Z = -P_X, \tag{2.6b}$$

$$-\tfrac{1}{2}W + (U - \tfrac{1}{2}X)W_X + (V + \tfrac{1}{2}Y)W_Y + (W - \tfrac{1}{2}Z)W_Z = -P_Z \tag{2.6c}$$

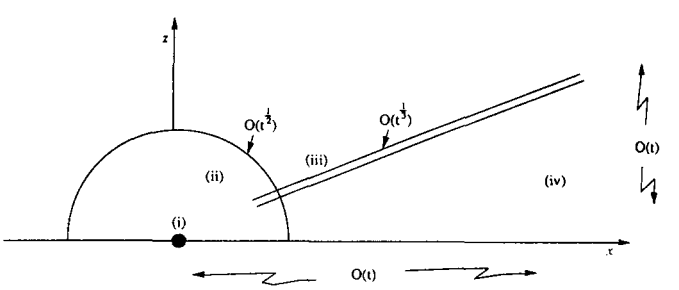

Fig. 1. Flow structure in $x - z$ plan view (upper half only) at large times t, due to the initial disturbance (i), including the $O(t^{1/2})$ elliptic zone (ii) (see §2), the edge layer (iii), near the wing tip of the spot (see §§3, 4), and the $O(t)$ sized region (iv) further downstream (see §6) where length scales of $O(1)$ in x, z are also induced. Compare Fig. 4.

from (2.1a, b, d), (2.4a), (2.5) with (2.1c) confirming that $\partial P/\partial Y$ must be zero; the main boundary conditions are

$$V=0 \text{ at } Y=0 \tag{2.6d}$$

$$U \sim Y + A(X,Z), \quad W \to 0, \quad \text{as } Y \to \infty, \tag{2.6e}$$

from (2.2c) and matching between the expansions (2.4a, b) respectively, with the constant λ_B normalized to unity; and the unknown displacement effect present in (2.6e) is related to the unknown surface pressure via the double Cauchy–Hilbert integral

$$P(X,Z) = -\frac{1}{2\pi} \int_{-\infty}^{\infty} \int_{-\infty}^{\infty} \frac{A_{\xi\xi}(\xi,\phi)\,d\xi\,d\phi}{[(X-\xi)^2+(Z-\phi)^2]^{1/2}}, \tag{2.7}$$

because of the potential-flow properties induced by (2.4c) with (2.1a–d) and the matching with (2.4b). An alternative formulation for the pressure-displacement interaction is in terms of the pressure in the outermost layer, satisfying

$$(\partial_X^2 + \partial_{\bar{y}}^2 + \partial_Z^2)\bar{p} = 0, \tag{2.8a}$$

$$\bar{p} \to P(X,Z), \quad \bar{p}_{\bar{y}} \to A_{XX}(X,Z), \quad \text{as } \bar{y} \to 0+, \tag{2.8b}$$

$$\bar{p} \to 0 \tag{2.8c}$$

in the farfield, in view of (2.4b, c), (2.2a). Hence we are left with the task of solving the nonlinear simularity inviscid-boundary-layer-like system (2.6a–e), subject to the interaction law (2.7) or (2.8a–c), for the $O(t^{1,2})$ zone properties. The theory and allied computations below are concerned mostly with the "trailing edge" of the spot, where the coordinates X, Z are typically large and positive, between the $O(t^{1,2})$ and $O(t)$ zones downstream: see the discussion of the latter in §6.

Other contexts for the nonlinear initial-value problem are described by Doorly and Smith [29], Smith [31], but that in (2.1)–(2.8) is the principal one. We move on next to consider the lowest level of input or evolved amplitude that will produce a significant nonlinear response in the spot trailing edge, before tackling higher levels in later sections.

3. Amplitude level I

Order-of-magnitude and matching arguments imply that the expansion of the flow solution at relatively large distances $X \gg 1$, $Z \gg 1$ downstream in the edge layer astride $Z \approx \mu X$ takes the underlying form

$$U = X\bar{Y} + X^{-1/3}(Eu_0 + \text{c.c.}) + \cdots + X^{-1}u_m + \cdots, \tag{3.1a}$$

$$V = X^{5/3}(Ev_0 + \text{c.c.}) + \cdots + v_m + \cdots, \tag{3.1b}$$

$$W = X^{-1/3}(Ew_0 + \text{c.c.}) + \cdots + X^{-1}w_m + \cdots, \tag{3.1c}$$

for the velocity components and

$$P = X^{2/3}(Ep_0 + \text{c.c.}) + \cdots + X^{-2/3}p_m + \cdots , \tag{3.1d}$$

$$A = X^{-1/3}(EA_0 + \text{c.c.}) + \cdots + X^{-1}A_m + \cdots , \tag{3.1e}$$

for the pressure and displacement respectively. An expansion similar to (3.1d) holds for the outer pressure $\bar{p}$. The direction factor $\mu = 8^{-1/2}$, while $\bar{Y} = X^{-1}Y$, $Z - \mu X = X^{-1/3}\eta$, and the dominant fluctuating part (subscript zero) at this stage has

$$E = \exp[\mathrm{i}(b_1 X^2 + \lambda X^{2/3}\eta)] , \tag{3.2}$$

where $b_1 = 3^{3/2}/16$, $\lambda = (3/8)^{1/2}$. The subscript m refers to the (real) mean-flow corrections, and c.c. denotes the complex conjugate. The unknown velocity coefficients u_0, u_m, etc. depend only on $\bar{Y}$, η, while p_n, A_n are unknown functions of η alone, with the explicit E-dependence as shown. The arrangement of the powers of E in the terms above is partly due to the nonlinear effects present and partly to the wave-like dependence in E. The coordinates $\bar{Y}$, η are $O(1)$. The successive determination of the various wave and mean-flow contributions then follows from substitution of (3.1) into (2.6), together with additional terms that arise.

The nonlinear interaction in this stage has the effects of the higher harmonics E^n, $|n| \geqslant 2$, being negligible and so it is dominated by interplay between the fundamental fluctuations $E^{\pm 1}$ and the mean-flow correction E^0. The strength of this interplay is due physically to the relative slowness of the mean-flow variations; a similar phenomenon also arises in the next section. In the present stage, incorporating the modification suggested in Smith (31, p. 158), the governing equations of concern are found, after working through several orders, to be

$$(p_0'' - \eta p_0)' = \mathrm{i}A_m p_0 , \tag{3.3}$$

$$-|p_0|^2 = \frac{1}{\pi}\int_{-\infty}^{\infty} \frac{A_m'(q)\,\mathrm{d}q}{\eta - q} , \tag{3.4}$$

in normalised form, controlling the complex wave part p_0 and the mean part A_m, with $|p_0|$ to tend to zero at large $|\eta|$. Here (3.4) stems from a combination of the outer interaction law (2.7) (or (2.8)) for the mean-flow components A_m, p_m and the relation $p_m \propto -|p_0|^2$ obtained from the mean components of the two momentum equations, while (3.3) represents modulation of the wave amplitudes [u_0, v_0, w_0, A_0, all proportional to p_0] due to the existence of the mean-flow correction. The critical layer and wall layer also present merely play a secondary role. At lower amplitudes, A_m is relatively small and so (3.3) reduces to Airy's equation for the wave part, in line with Doorly and Smith [29] and the classical linear theory of caustics, and (3.4) then provides only a small correction determining the mean-flow (vortex) response A_m, with little feedback. At $O(1)$ amplitudes, the fast-fluctuation/slow-mean-flow nonlinear mechanism becomes fully active, and computations of the nonlinear system (3.3), (3.4) are necessary, sample solutions being presented in Fig. 2. These agree with the Airy form at reduced amplitudes. At relatively high amplitudes however a novel structure is suggested to emerge, as follows.

When $|A_m|$ becomes large, the typical scale of $|\eta|$ expands, like Δ say (with $|A_m| \sim \Delta^{3/2}$), $|p_0|$ also grows, like $\Delta^{1/4}$, and (3.3), (3.4) then yield the system

$$h^3 + \tilde{\eta}h = -a_m , \tag{3.5}$$

$$(3h^2 + \tilde{\eta})r' + (3hh' + 1)r = 0\,, \tag{3.6}$$

$$-r^2 = \frac{1}{\pi}\int_{-\infty}^{\infty} \frac{a_m'(q)\,\mathrm{d}q}{\tilde{\eta} - q}\,. \tag{3.7}$$

Here $p_0 \sim \Delta^{1/4} r \exp[\mathrm{i}\Delta^{3/2} f + O(1)]$ and $A_m \sim \Delta^{3/2} a_m$ with the amplitude r, the phase f and the mean part a_m all being generally $O(1)$ real functions of the new $O(1)$ coordinate $\tilde{\eta} \equiv \Delta^{-1}\eta$, and $h \equiv \mathrm{d}f/\mathrm{d}\tilde{\eta}$. The increasing variation in phase is especially noteworthy. Analysis of (3.5)–(3.7) implies that there exists just a single acceptable phase branch for $h(\tilde{\eta})$, as opposed to the two that exist in linear theory and to the three that (3.5) alone would indicate for a given $a_m(\tilde{\eta})$. This single branch is currently believed to have h smooth for all $\tilde{\eta}$, and a sample numerical solution of (3.5)–(3.7) is given in Fig. 3. At these amplitudes the function a_m is negative except at quite large positive $\tilde{\eta}$. So the mean-flow correction comprises relatively long vortices such that the mean displacement increment is mostly *positive* except outside the spot where it is negative. Also, the fluctuating components

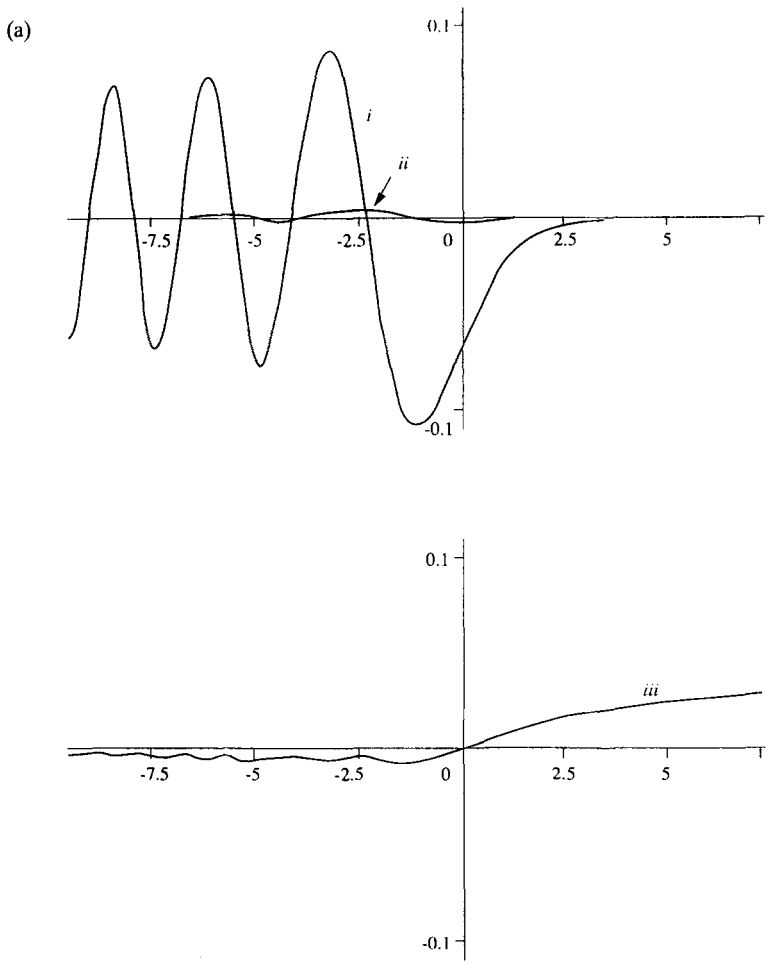

Fig. 2. Solutions computed for the wave contribution p_0 (real part i, imaginary part ii) and the mean contribution A_m (iii), at two amplitudes within level I: (a) small, (b) of order unity. Note the changes of scale, and of phase, and the square-root growth of A_m as $\eta \to \infty$.

(b)

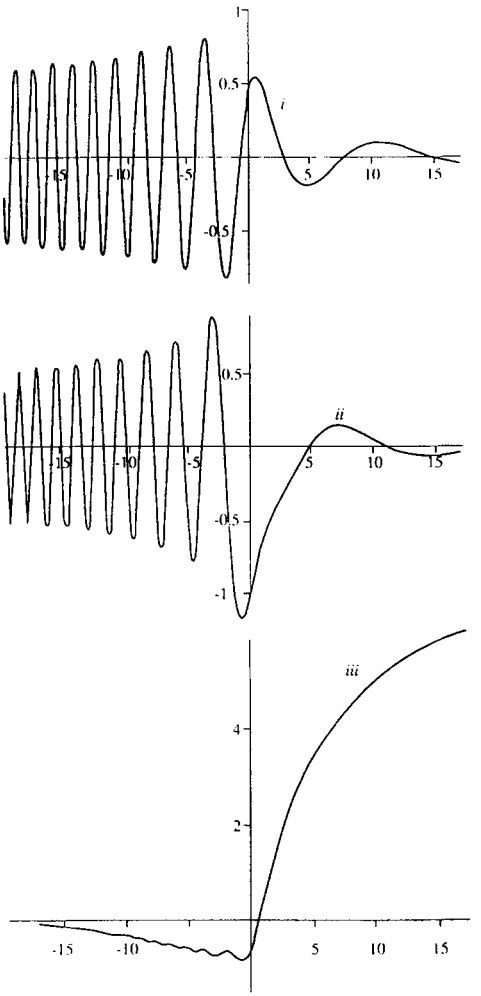

Fig. 2. (Continued).

have their positions of maximum amplitude gradually being moved towards the middle of the spot's trailing edge. The large-Δ theory here points to the new interactive structure that comes into play next at an increased amplitude level.

4. Amplitude level II

Significant changes are found to occur first when the amplitudes increase (slightly) to the stage where $Z-\mu X$ becomes of order unity. That corresponds formally to Δ above rising to the order $X^{1/3}$, yielding estimates for the new orders involved here.

The expansions now holding therefore have $Z-\mu X=\hat{\eta}$ being of $O(1)$, as is $\bar{Y}$, and

$$U = X\bar{Y} + X^{-1/4}(\hat{E}\hat{u}_0 + \text{c.c.}) + \cdots + X^{-1/2}\hat{u}_m + \cdots, \tag{4.1a}$$

$$V = X^{7/4}(\hat{E}\hat{v}_0 + \text{c.c.}) + \cdots + X^{1/2}\hat{v}_m + \cdots, \tag{4.1b}$$

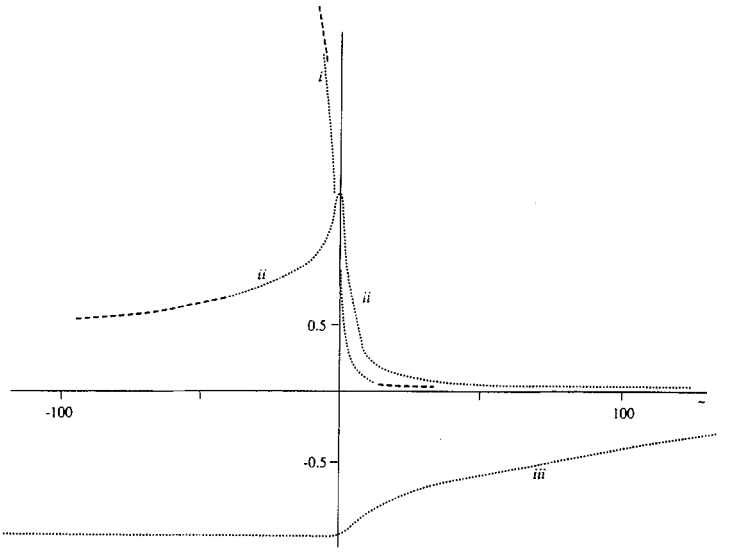

Fig. 3. Numerical solutions for the increased-amplitude response of (3.5)–(3.7), corresponding to the upper extreme of level I or the lower extreme of level II: (i) h, (ii) r, (iii) a_m. Dashed curves denote farfield asymptotes.

$$W = X^{-1/4}(\hat{E}\hat{w}_0 + \text{c.c.}) + \cdots + X^{-1/2}\hat{w}_m + \cdots, \tag{4.1c}$$

$$P = X^{3/4}(\hat{E}\hat{p}_0 + \text{c.c.}) + \cdots + X^{-1/2}\hat{p}_m + \cdots, \tag{4.1d}$$

$$A = X^{-1/4}(\hat{E}\hat{A}_0 + \text{c.c.}) + \cdots + X^{-1/2}\hat{A}_m + \cdots, \tag{4.1e}$$

c.f. (3.1a–e), with $\bar{p}$ having an expression similar to (4.1d). The primary fluctuating part here is given by

$$\hat{E} = \exp[\mathrm{i}(b_1 X^2 + \lambda X\hat{\eta} + X^{1/2}\hat{f}(\hat{\eta}))], \tag{4.2}$$

because of the enhanced phase variation, here the unknown function $\hat{f}(\hat{\eta})$. The main new contributions in this stage come from extra inertial effects in the momentum balances for the mean-flow correction, in (4.3c) below. Apart from that, the dominance of the (long/short) interaction between the fundamental fluctuations and the mean flow stays intact.

Substitution of (4.1), (4.2) into (2.6)ff and integration in $\bar{Y}$ yields eventually the new controlling equations for the unknown wave amplitude $\hat{p}_0$, mean correction $\hat{A}_m$ and phase term $\hat{f}$, in the normalised form

$$\hat{f}'^3 + 2\hat{\eta}\hat{f}' - \hat{f} = \hat{A}_m, \tag{4.3a}$$

$$(\hat{\eta} + a_2\hat{f}'^2)(|\hat{p}_0|)' + (\tfrac{1}{4} + a_2\hat{f}'\hat{f}'')|\hat{p}_0| = 0, \tag{4.3b}$$

$$-\tfrac{1}{2}\hat{A}_m - \hat{\eta}\hat{A}_m' - (|\hat{p}_0|^2)' = \frac{1}{\pi}\int_{-\infty}^{\infty} \frac{\hat{A}_m''(\hat{q})\,\mathrm{d}\hat{q}}{\hat{\eta} - \hat{q}}. \tag{4.3c}$$

The constant a_2 is positive. It is seen that (4.3a–c) are analogous with (3.5)–(3.7) in turn, with the two extra inertial effects in (4.3c)'s left-hand side being evident. Solutions for the

current level II are presented by Dodia et al. [39]. At reduced amplitudes the match is achieved with the level-I description in the previous section, as expected. For sufficiently enhanced amplitudes II, at the opposite extreme, the influence of the integral contribution in (4.3c) is believed to die out, signalling a diminution of the mean-flow effect produced by the motion near the external stream.

Thus $\hat{A}_m$ typically becomes of order $\hat{\Delta}^{3/2}$(large) then, with the $\hat{\eta}$-scale expanding like $\hat{\Delta}$ and $|\hat{f}|$, $|\hat{p}_0|$ increasing like $\hat{\Delta}^{3/2}$, $\hat{\Delta}^{5/4}$. As a result, (4.3a, b) remain in full, at large amplitudes, but (4.3c) reduces to

$$-\tfrac{1}{2}\hat{A}_m - \hat{\eta}\hat{A}'_m = (|\hat{p}_0|^2)' \,. \tag{4.4}$$

This reflects a balance between the mean-flow momentum, near the wall, and the Reynolds-stress effects there due to the amplitude-squared inertia from the main fluctuations. The balance contrasts with that in (3.7) for instance. [Solutions of (4.4) with (4.3a, b) are given in the last reference and are analogous with those described later in §8]. The next move is to consider the new stage that must arise as the amplitude level continues to increase. The new stage occurs when the whole of the trailing-edge region becomes affected by nonlinearity, i.e. the typical $Z - \mu X$ value rises to $O(X)$, corresponding to $\hat{\Delta}$ increasing dramatically to $O(X)$ in effect. Then $|\hat{A}_m|$ increases to $O(X^{3/2})$, as does $|\hat{u}_m|$ since they are proportional, and so the mean-flow correction becomes comparable with the basic mean flow [$X\bar{Y}$ in (4.1a)], formally. In consequence, a strongly nonlinear effect is implied at that level, with the fluctuating part $\propto X^{-1/4}\hat{A}_0$ also increasing to the order X since $|\hat{A}_0| \propto |\hat{p}_0| \sim X^{5/4}$ then. This is investigated below.

5. Amplitude level III, affecting the entire trailing-edge

Here the characteristic amplitude level for both the fluctuating and the mean-flow parts is raised to $O(X)$, as far as the velocities U, W and the negative displacement A are concerned, with corresponding increases in V, P, as inferred from the previous level II. The nonlinear interactions present now become *strongly nonlinear* however and effectively all the higher harmonic fluctuations also play a significant role, as follows. Since Z- and X-variations are comparable when the whole of the trailing-edge region is considered, we work in terms of the polars R, θ, where $(X, Z) = R(\cos\theta, \sin\theta) = R(c, s)$, and now θ is $O(1)$ typically with R being large. Hence the flowfield solution has

$$\bar{U} = R(\bar{U}_m + \bar{U}_f) + \cdots, \tag{5.1a}$$

$$V = R^3\bar{V}_f + R(\bar{V}_m + \bar{\bar{V}}_f) + \cdots, \tag{5.1b}$$

$$\bar{W} = R(\bar{W}_m + \bar{W}_f) + \cdots, \tag{5.1c}$$

$$P = R^2\bar{P}_f + (\bar{P}_m + \bar{\bar{P}}_f) + \cdots, \tag{5.1d}$$

$$A = R(\bar{A}_m + \bar{A}_f) + \cdots. \tag{5.1e}$$

The relative error in (5.1) is $O(R^{-2})$ throughout and, again for convenience, $\bar{U}$, $\bar{W}$ are

the R-, θ-velocities, so that $U = \bar{U}c - \bar{W}s$, $W = \bar{U}s + \bar{W}c$ and, for example, $(\bar{U}, \bar{W}) \sim (Y + A)(c, -s)$ at large Y from (2.6e). In the above the subscripts m, f refer to the mean parts and the fluctuating parts respectively, the latter having zero mean. The *total* mean flow, e.g. $\bar{U}_m$, is unknown now but it varies slowly, being dependent on $\bar{Y}$, θ, whereas the unknown fluctuations, e.g. $\bar{U}_f$, depend also on the rapid variable $F \equiv b(\theta)R^2$ and represent in effect Fourier series in F. The phase function $b(\theta)$ has also to be found.

The main controlling equations from combining (5.1) with (2.6)ff are

$$2b\frac{\partial \bar{U}_f}{\partial F} + \frac{\partial \bar{V}_f}{\partial \bar{Y}} + b'\frac{\partial \bar{W}_f}{\partial F} = 0\,, \tag{5.2a}$$

$$2(\bar{U}_m + \bar{U}_f - \tfrac{1}{2})b\frac{\partial \bar{U}_f}{\partial F} + \bar{V}_f\frac{\partial}{\partial \bar{Y}}(\bar{U}_m + \bar{U}_f) + (\bar{W}_m + \bar{W}_f)b'\frac{\partial \bar{U}_f}{\partial F} = -2b\frac{\partial \bar{P}_f}{\partial F}\,, \tag{5.2b}$$

$$2(\bar{U}_m + \bar{U}_f - \tfrac{1}{2})b\frac{\partial \bar{W}_f}{\partial F} + \bar{V}_f\frac{\partial}{\partial \bar{Y}}(\bar{W}_m + \bar{W}_f) + (\bar{W}_m + \bar{W}_f)b'\frac{\partial \bar{W}_f}{\partial F} = -b'\frac{\partial \bar{P}_f}{\partial F}\,, \tag{5.2c}$$

nominally for the dominant fluctuations, coupled with a similar but forced linearized system for the fluctuation corrections and with the nonlinear system

$$2\bar{U}_m - \bar{Y}\frac{\partial \bar{U}_m}{\partial \bar{Y}} + \frac{\partial \bar{V}_m}{\partial \bar{Y}} + \frac{\partial \bar{W}_m}{\partial \theta} = 0\,, \tag{5.3a}$$

$$-\tfrac{1}{2}\bar{U}_m + (\bar{U}_m - \tfrac{1}{2})\left(\bar{U}_m - \bar{Y}\frac{\partial \bar{U}_m}{\partial \bar{Y}}\right) + (\bar{V}_m + \tfrac{1}{2}\bar{Y})\frac{\partial U_m}{\partial \bar{Y}} + \bar{W}_m\left(\frac{\partial \bar{U}_m}{\partial \theta} - \bar{W}_m\right) = \bar{S}_1\,, \tag{5.3b}$$

$$-\tfrac{1}{2}\bar{W}_m + (\bar{U}_m - \tfrac{1}{2})\left(\bar{W}_m - \bar{Y}\frac{\partial \bar{W}_m}{\partial \bar{Y}}\right) + (\bar{V}_m + \tfrac{1}{2}\bar{Y})\frac{\partial \bar{W}_m}{\partial \bar{Y}} + \bar{W}_m\left(\frac{\partial \bar{W}_m}{\partial \theta} + \bar{U}_m\right) = \bar{S}_2\,, \tag{5.3c}$$

holding for the mean flow. Here $\bar{Y}$ stands for $R^{-1}Y$ and is comparable with the previous $\bar{Y}$, while $\bar{S}_1$, $\bar{S}_2$ are Reynolds stress terms which can be shown to be proportional to the square of the typical amplitudes of the dominant fluctuations. Likewise, a part of the fluctuation-correction system mentioned above can be shown to yield a compatability relation (CR, say) between the mean flow and the dominant fluctuations. Consequently, (5.2a–c) [with the appropriate $\bar{P}_f$–$\bar{A}_f$ law derived from (2.7) or (2.8)], CR and (5.3a–c) are found to provide overall a closed nonlinear system controlling the major unknowns, namely the dominant fluctuations, the total mean flow, and the phase function $b(\theta)$.

These and other features of this level-III interaction are currently being studied: Bowles et al. [40]. Clearly the part (5.2a–c) can be simplified somewhat by taking the skewed velocity component $(2b\bar{U}_f + b'\bar{W}_f)$ and combining (5.2b, c). If also the skewed mean flow is assumed to maintain a uniform shear, as in the previous two sections, then (5.2a–c) lead to a travelling-wave form of the Benjamin–Ono equation, for the dependence of $\bar{A}_f$ on F, thus verifying the existence of nonlinear multiple waves. Corresponding simplifications occur in the other parts of the overall system. One notes also that the mean pressure gradient has negligible influence now (see (5.3b, c)), and likewise for the mean contribution in the interaction with the external stream. Again, at reduced amplitudes the necessary merging with level II is obtained. The behaviour at increased amplitudes in level III is expected to

involve more concentration of the spot's spread, as 3D longitudinal vortex strength increases; see Bowles et al. [40].

6. The spot centre

In the main body of the spot, at larger distances $x \sim t$ downstream, the full Euler equations (2.1) appear to come back into play, from the following reasoning. Formally the scaled distances X, Z, and hence R, then tend to $O(t^{1/2})$, to make x, z be of order t. It follows that the y-scale that was originally $t^{-1/2}$ in the lowest layer of (2.4a), but is then enhanced by a factor $O(R)$ in §§3–5, rises to $O(1)$. Simultaneously, the uppermost y-scale behaves as $t^{1/2}R^{-1}$ typically (see (2.4)ff), because of the fast E, $\hat{E}$ or F variations in §§3–5, and so it also tends to $O(1)$ as R increases to the order $t^{1/2}$, while the y-scale of the middle layer in (2.4b) stays $O(1)$. Therefore the three-layer structure described in §2 collapses into a single structure. Along with this, the characteristic variation of the fluctuating parts, with respect to x, z, becomes faster due to the rapid F (or E, $\hat{E}$) dependence, essentially by a length factor of order R^{-1}, or $t^{-1/2}$ now; derivatives involving F are greater than those not involving F by a factor $O(R^2)$. This implies that the characteristic length scale in x, z falls to $O(1)$ as far as the fluctuations are concerned. Again, the strong nonlinearity encountered in §5 points to strong nonlinearity persisting as the $x = O(t)$ zone is entered downstream. For example, the velocity u becomes $O(1)$ then, from (2.4) with (5.1a, c). All the above leads to the full unsteady 3D Euler system, then, holding in the centre of the spot, and implying a large numerical task of course.

That is not the whole story, however. For, according to §5, there is significant interplay between those fast fluctuations and the more slowly varying total mean flow. So there must be extra length scales in operation, specifically lengths x, z of $O(t)$ in fact [from reasoning as in the previous paragraph], in addition to the $O(1)$ length scales above. The extra length scales are associated predominantly with the equations for the mean flow (slender-flow equations, cf. (5.3)) and they must play an equally important role, linking the main short- and long-scale behaviour in similar fashion to the links discussed in §5.

Moreover, as the spot continues even further downstream, to distances x, z of order $\mathrm{Re}^{1/2}$ measured from the initial disturbance [i.e. global distances $\bar{x}$, $\bar{z}$ of $O(1)$, since $(\bar{x}, \bar{z}) = \mathrm{Re}^{-1/2}(x, z)$], the two interacting short and long length scales above become $O(\mathrm{Re}^{-1/2})$ and $O(1)$ respectively, in the global coordinates $\bar{x}$, $\bar{z}$, with the normal coordinate staying $O(\mathrm{Re}^{-1/2})$. These scalings appear to be physically sensible. A new feature arises then, however, since viscous forces must affect the mean-flow equations on the $\bar{x}$, $\bar{z} \sim 1$ scale. Indeed, the 3D boundary-layer equations are implied,

$$\bar{u}_{\bar{x}} + \bar{v}_y + \bar{w}_{\bar{z}} = 0\,, \tag{6.1a}$$

$$\bar{u}_{\bar{t}} + \bar{u}\bar{u}_{\bar{x}} + \bar{v}\bar{u}_y + \bar{w}\bar{u}_{\bar{z}} = \bar{s}_1 - \bar{p}_{\bar{x}} + \bar{u}_{yy}\,, \tag{6.1b}$$

$$\bar{w}_{\bar{t}} + \bar{u}\bar{w}_{\bar{x}} + \bar{v}\bar{w}_y + \bar{w}\bar{w}_{\bar{z}} = \bar{s}_2 - \bar{p}_{\bar{z}} + \bar{w}_{yy}\,, \tag{6.1c}$$

essentially for the unknown mean-flow velocities $(\bar{u}, \bar{v}, \bar{w})(\bar{x}, y, \bar{z}, \bar{t})$, where $\bar{t} \equiv \mathrm{Re}^{1/2}t$ denotes the global time. Here $\bar{p}(\bar{x}, \bar{z}, \bar{t})$ is the prescribed external-stream pressure, associated with $(\bar{u}, \bar{w}) \to (u_e, w_e)(\bar{x}, \bar{z}, \bar{t})$ say, as $y \to \infty$, whereas $\bar{s}_1$, $\bar{s}_2$ are the unknown

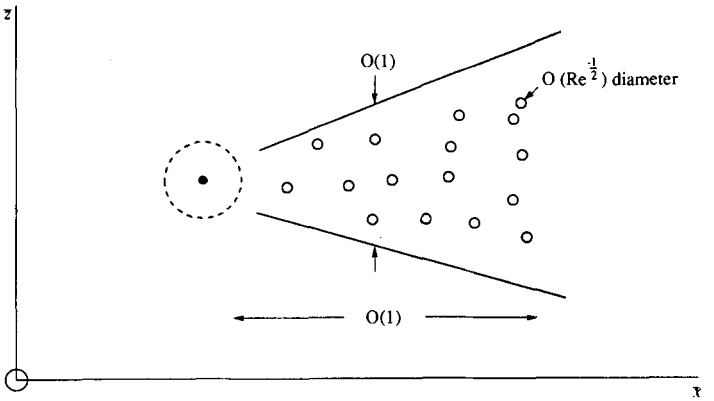

Fig. 4. Spot flow structure at much later times, i.e. global $\bar{t}$ of order unity, showing the $O(1) \times O(1)$ global region governed by the 3D boundary-layer equations and the $O(\mathrm{Re}^{-1/2}) \times O(\mathrm{Re}^{-1/2})$ small Euler regions inside. The regions are linked together as described in §6, with their common normal scale being $O(\mathrm{Re}^{-1/2})$. Sub-scales are discussed in §7.

Reynolds stress terms (cf. (5.3b, c)) comprising nonlinear effects from the fluctuating velocity components governed by (2.1). The full interaction between (6.1), (2.1) also involves the mean profile $\bar{u} = u_B$ in (2.2b), which is now dependent on $\bar{x}$, y, $\bar{z}$, $\bar{t}$ and unknown, as is the corresponding nonzero $\bar{w} = w_B$ in general. It is intriguing that, according to the above argument, the flow properties on those two length scales remain fully interactive, with the viscous 3D boundary-layer system (6.1) and the inviscid 3D Euler system (2.1) being coupled together via the Reynolds stresses in (6.1b, c) and the profiles in (2.2). See Fig. 4, and observe that interference is assumed negligible from the elliptic $O(\mathrm{Re}^{-1/4})$ zone that was originally the $O(t^{1/2})$ zone, lying behind the spot and surrounding the initial station.

As with other aspects, the present area seems to merit much further research. The impact of high-amplitude analysis for example, mentioned near the end of the previous section, remains to be studied here. In addition to the above broader-scale behaviour, however, there are finer-scale responses to consider, as in the following section.

7. Internal dynamics and viscous effects

The major element missing so far in the above theory is viscosity, which substantially governs the finer-scale dynamics and the connection with larger scales, apart from the interesting global-scale effect predicted in (6.1)ff. Although our concern in the majority of this article is with global features, we also consider the internal features briefly below, more details and description being given in the references cited.

An important role is played by the 3D viscous sublayer or sublayers lying (initially) between the mainly inviscid regions studied in Sections 2–6 and the solid surface. The sublayer is neglected above, as it is assumed to remain relatively thin and secondary, and that seems likely to stay entirely true for the first stages I, II addressed in Sections 3, 4. At higher amplitudes such as III however the sublayer, which initially occupies only a small fraction $O(\mathrm{Re}^{-1/4})$ of the complete boundary layer, is governed by the classical non-interactive unsteady 3D boundary-layer formulation [(6.1) in effect, without the Reynolds-stress terms] holding beneath the Euler form of (2.1). Hence the sublayer is subjected to

strong unsteady pressure gradients, including adverse ones, produced by the strongly nonlinear inviscid behaviour in III for instance. First thoughts would suggest that, under such prescribed pressure gradients, the sublayer is likely to erupt in the sense of its solution becoming singular within a finite time in the Van Dommelen [41] fashion, such that

$$\delta_1 \to \infty \quad \text{as } t \to t_1^- \,. \tag{7.1}$$

Here δ_1 is the usual scaled sublayer displacement thickness, the singular time t_1 is finite, and (7.1) occurs locally at a particular x station; see the structure involved in Elliott et al. [42]. The singularity is especially relevant if the inviscid Euler behaviour predicted by (5.2)–(5.3) or (2.1) becomes extreme in its amplitude variation. Again, (7.1) is written as if for 2D flow but the 3D case appears to be predominantly quasi-2D anyway (Elliott et al. [42], Cowley et al. [43]). More significantly, the flow solution next moves into shorter length and time scales until inner-outer interaction takes place between the increasing displacement (effectively δ_1) and the induced pressure due to back-influence from the inviscid slip stream outside, as described by Elliott et al. [42]. At that stage the work of Brown et al. [44] comes into play, implying a further and stronger singularity in the displacement as well as in the local pressure, and hence yet newer physics enters the reckoning. Recent theoretical and computational studies of that stage have been made by Cassel et al. [45], with F.T.S. extending the work to 3D.

Further thought however points to the finite-time break-up of Smith [37] as being more likely to arise in practical as well as theoretical terms. This nonlinear break-up singularity is associated with inner-outer *interaction* affecting the sublayer and such interaction is always present. The break-up occurs at a time (t_2 say) earlier than the non-interactive time t_1, since the nonlinear break-up criterion of the last reference is met earlier. See Cassel et al. [45]. The break-up involves the local response

$$|\partial p/\partial x| \to \infty \,, \quad \tau_W \to \infty \,, \quad \text{as } t \to t_2^- \tag{7.2}$$

in particular, with the pressure remaining finite but the pressure gradient and the normalised wall shear stress τ_W becoming infinite in anticipation of a change of scale. The break-up (7.2) is followed by the entry of new physical effects locally, corresponding to the creation of significant normal pressure gradients and nonlinear critical-layer interaction, on a shorter time scale: Hoyle et al. [34]. After that the flow may enter a stage of temporary or permanent roll-up of a local vortex, as suggested in the last reference. Studies of these further stages are in progress, at least for 2D motion, while the extension to 3D is started in Hoyle [46], Hoyle and Smith [47] and is currently being continued.

Agreement between the theory for (7.2) and accurate computations is found to be close, as Peridier et al. [36] show. Agreement between the theory and experiments is also reasonably close, as discussed by Smith and Bowles [48] for the Nishioka et al. [49] experiments on the first spike in transition. The nonlinear criterion for the first spike has the integral form

$$\int_0^\infty (\bar{u} - c)^{-2} \, \mathrm{d}y = 0 \tag{7.3}$$

in essence, according to the theory in Smith [37], where $\bar{u}(y, t)$ denotes the local velocity profile in the sublayer and c is the inflexional velocity; the criterion (7.3) is near to being

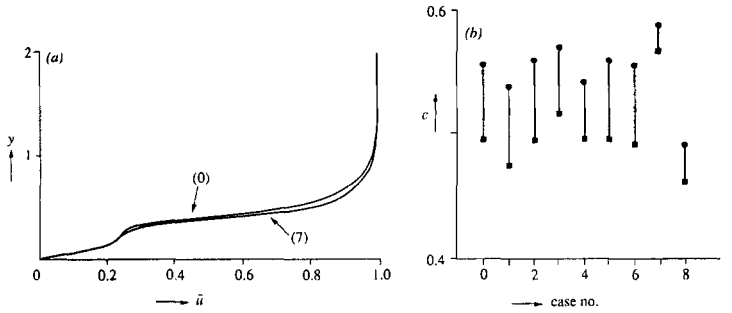

Fig. 5. Comparisons between theory (Smith and Bowles [48]) and experiment (Nishioka et al. [49]) concerning the nonlinear criterion (7.3) and the first transitional spike. Explanation of the cases 0–8 is given in the former reference.

satisfied by the experimental profiles as Fig. 5 shows. Both the theoretical-computational and the theoretical-experimental comparisons are encouraging aspects.

Finite-time break-up must occur sooner or later, then, and much further work is called for to understand more fully the impact of these internal eruptive or bursting processes on the larger-scale Euler evolution addressed in Sections 2–6 and the generation of faster time and length scales and hence higher frequency and wavenumber spectral content. There is in particular the issue of whether, or not, a clear link can be established with the formation of hairpin vortices in reality, the observed hierarchy of scales, and the so-called turbulence reproduction cycle (see 'domino process' earlier), near the surface: e.g. C.R. Smith et al. [8], Grass et al. [50] and references therein. Certainly, (viscous induced) eruptions as in (7.1), (7.2) can also take place in other scales, both larger as in the context of (6.1) and smaller, cf. the cascade process described by Smith et al. [33] which predicts the scales

$$O(\mathrm{Re}^{-1} \ln \mathrm{Re}) , \tag{7.4}$$

$$O(\mathrm{Re}^{-3/4}) , \tag{7.5}$$

for the final turbulent sublayer thickness and the microscale of the mid-flow respectively, in agreement with common turbulence models and the Kolmogorov estimate in turn.

8. Further applications, comparisons and comments

This area of research, on which work done and work in progress have both been reviewed above, is felt to be in an interesting and challenging state as regards both the global and the internal properties considered theoretically above for nonlinear spots. The strong more global nonlinearity encountered in Sections 5, 6 is particularly exciting as is that in Section 7 for the more internal flow features. We would especially highlight the novel interaction that arises on the largest scale (airfoil scale) as covered by (6.1) coupled with (2.1). The highest amplitudes tackled so far, in Sections 5, 6, require concerted further study however. A point of interest here is that an alternative to (5.1), with only small $O(R^{-1})$ mean-correction and small wave terms in A for example, also seems consistent on the face of it, thus reinforcing the need for such further study. A related point is that markedly different flow structures might be set up sufficiently far downstream of the initial disturbance as mentioned in Section

1, although there is little work in connecting these structures with an initial-value problem as here. Likewise, mention should be made of the near-planar case set up experimentally by Kachanov et al. [51], the 2D inviscid theory of which is much easier to handle, but our emphasis is on the 3D nonlinear development which represents the more common case. There is in fact a wide variety of scales present within the 3D spot evolution identified by the theory, agreeing with the description of "spots within spots", and the overall picture looks fairly encouraging and self-consistent as a basis for continuing study.

Channel flows and the broadly similar flows of wall jets are considered by Dodia [52]. In such flows the spot evolution has a form related to, but different from, that for the boundary-layer case of Sections 2–7. We shall be brief. The large-t response is distinct from (2.4), (2.5), and the pressure-displacement law alters from (2.7). Hence it is found that level I is by-passed and the amplitude level II of §4 is encountered immediately, as the first nonlinear stage. The same scalings as in §4 apply except that $\hat{E}$ in (4.2) needs modifying slightly, with $X^{3/2}$ replacing X^2, among other things. The solutions during that amplitude level and their growth in the large-$\hat{\Delta}$ extreme corresponding to (4.4) are presented by Dodia [52]. Beyond that, e.g. at level III, the spot flow structure, expansions and controlling equations are believed to become essentially the same as for the boundary-layer case, partly because the mean pressure-displacement law then plays only a passive role.

Concerning mainly boundary layers again, the theory tentatively appears to fall in line with all the experimental findings (a)–(e) summarized in §1, it is believed, in a qualitative or quantitative sense. The finding (e) concerning the sharp front and edges of the spot, and trailing wave packets, has not been touched upon specifically in this article, but it is discussed by Smith et al. [33], Smith [31] and partly by Kachanov et al. [51], while the findings (a)–(d) are all implicit in the present theory. On the other hand, agreement with experiments is poor so far for the spot spreading rate (in plan view), although this may change once solutions for the amplitude level III and beyond (§§5–7) are obtained. On more global features (§§2–6), some qualitative agreement with experiments and computations is demonstrated in Smith [30] for the initial-value problem (2.1) alone, while Kachanov et al. [51] find surprisingly good agreement with experiments carefully controlled to remain 2D for a long way downstream. On the more internal features quantitative agreement with computations and experiments has been noted in §7 and in Fig. 5. In another but related context, Fig. 6 shows

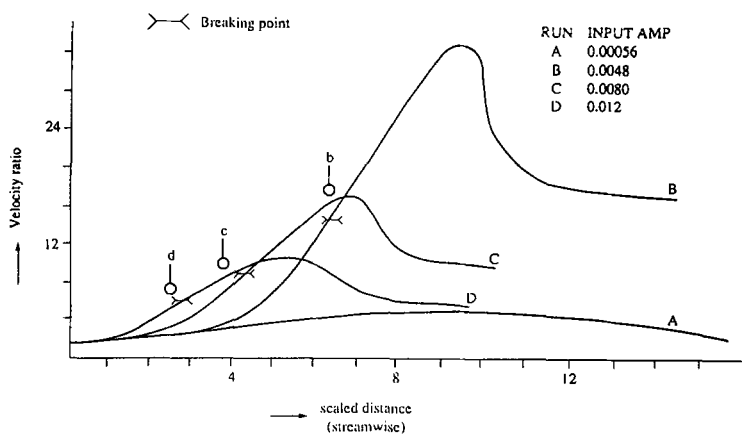

Fig. 6. Comparisons concerning the origins of turbulent spots in forced transition, for slightly 3D input upstream. Theoretical (Stewart and Smith [53]) blow-up locations b, c, d are compared with the 'breaking-point' locations found experimentally (Klebanoff and Tidstrom [54]) in the runs B, C, D.

quantitative comparisons between nonlinear theory in Stewart and Smith [53] and experiment in Klebanoff and Tidstrom [54] with regard to the so-called breaking point found downstream of a slightly 3D (maintained) input in the experiments. The comparisons are again close. The breaking point here signals the onset of turbulent spots in the subsequent flow, linking with the type of spot considered hitherto in this article. Additional points of firm agreement on the above and other major features of transitional/turbulent spots remain to be secured, of course, especially concerning §§2–6 as Smith [31] mentions in some more detail, but the comparisons so far seem encouraging.

Support from SERC, U.K., for B.T.D. and R.G.A.B., and from ARO (contract no. DAAL03-92-G-0040) for F.T.S. is gratefully acknowledged, as are helpful comments by Prof. D.S. Henningson and a referee.

References

1. H.W. Emmons, The laminar-turbulent transition in a boundary layer, Part I. *J. Aeronaut. Sci.* 18 (1951) 490–498. (See also *J. Fluid Mech.* 9 (1963) 235–246.)
2. T. Katz, A. Seifert and I.J. Wygnanski, On the evolution of the turbulent spot in a laminar boundary layer with a favourable pressure gradient. *J. Fluid Mech.* 221 (1990) 1–22.
3. A. Glezer, Y. Katz and I.J. Wygnanski, On the breakdown of the wave packet trailing a turbulent spot in a laminar boundary layer. *J. Fluid Mech.* 198 (1989) 1–26.
4. J.J. Riley and M. Gad-el-Hak, The dynamics of turbulent spots. In *Frontiers in Fluid Mechanics* (ed. S.H. Davies and J.L. Lumley). New York, Springer-Verlag (1985) pp. 123–155.
5. A.E. Perry, T.T. Liu and E.W. Teh, A visual study of turbulent flows. *J. Fluid Mech.* 104 (1981) 387–405.
6. J.D.A. Walker, Wall-layer eruptions in turbulent flows. In *Proc. Second IUTAM Symp. on structure of turbulence and drag reduction* (ed. A. Gyr). New York: Springer (1990) pp. 109–117.
7. R.E. Falco, Structural aspects of turbulence in boundary layer flows. In *Proc. Sixth Biennial Symp. Turb.* (ed. J.K. Zakin and G.K. Patterson), ch. 1.1–1.4. University of Missouri-Rolla (1979).
8. C.R. Smith, J.D.A. Walker, A.H. Haidari and U. Sobrun, On the dynamics of near-wall turbulence. *Phil. Trans. R. Soc.* A336 (1991) 131–175.
9. M. Gad-el-Hak, R.F. Blackwelder and J.J. Riley, On the growth of turbulent regions in laminar boundary layers. *J. Fluid Mech.* 110 (1981) 73–95.
10. P.R. Bandyopadhyay, Aspects of the equilibrium puff in transitional pipe flow. *J. Fluid Mech.* 163 (1986) 439–458.
11. M.J. Lighthill, Introduction. Boundary layer theory. *Laminar boundary layers* (ed. L. Rosenhead), ch. II, Oxford University Press (1963).
12. H. Schlichting, *Boundary-layer theory*. 4th edn. McGraw-Hill (1979).
13. F.W. Chambers and A.S.W. Thomas, Turbulent spots, wave packets and growth. *Phys. Fluids* 26 (1983) 1160–1162.
14. I.J. Wygnanski, J.H. Haritonidis and R.E. Kaplan, On a Tollmien–Schlichting wave packet produced by a turbulent spot. *J. Fluid Mech.* 92 (1979) 505–528.
15. G.B. Schubauer and P.S. Klebanoff, Contributions on the mechanics of boundary layer transition. *NACA Rep. 1289* (1956).
16. M.R. Head and P. Bandyopadhyay, New aspects of turbulent boundary-layer structure. *J. Fluid Mech.* 107 (1981) 297–338.
17. A.V. Johansson, J. Her and J.H. Haritonidis, On the generation of high-amplitude wall-pressure peaks in turbulent boundary-layers and spots. *J. Fluid Mech.* 175 (1987) 119–142.
18. D.S. Henningson and P.H. Alfredson, The wave structue of turbulent spots in a plane Poiseuille flow. *J. Fluid Mech.* 178 (1987) 405–421.
19. S.K. Robinson, Coherent motions in the turbulent boundary layer. *Ann. Rev. Fluid Mech.* 23 (1991) 601–639.
20. A. Leonard, Turbulent structures in wall-bounded shear flow observed via three-dimensional numerical simulations. *Lect. Notes Phys.* Springer-Verlag, Berlin 136 (1981) 119–145.
21. E.T. Bullister and S.A. Orszag, Numerical simulation of turbulent spots in channel and boundary-layer flows. *J. Sci. Comput.* 2 (1987) 263–281.
22. D.S. Henningson, P. Spalart and J. Kim, Numerical simulations of turbulent spots in plane Poiseuille and boundary-layer flow. *Phys. Fluids* 30 (1987) 2914–2917.

23. D.S. Henningson and J. Kim, On turbulent spots in a plane Poiseuille flow, *J. Fluid Mech.* 228 (1991) 183–205.
24. A. Lundbladh and A.V. Johansson, Direct simulation of turbulent spots in plane Couette flow. *J. Fluid Mech.* 229 (1991) 499–516.
25. H. Fasel, Numerical solution of instability and transition in boundary-layer flows. In *Laminar-turbulent transition* (ed. D. Arnal and R. Michel). Berlin: Springer-Verlag (1990).
26. U. Konzelmann and H. Fasel, Numerical simulation of a three-dimensional wave packet in a growing flat plate boundary layer. In *Proc. R. Aeronautic. Soc.* Meeting on Transition, Cambridge, U.K. (1991).
27. D. Henningson, A. Lundbladh and A.V. Johansson, A mechanism for by-pass transition from localized disturbances in wall-bounded shear flows. *J. Fluid Mech.* 250 (1993) 169–207.
28. J. Cohen, K.S. Breuer and J.H. Haritonidis, On the evolution of a wave packet in a laminar boundary layer. *J. Fluid Mech.* 225 (1991) 575–606.
29. D.J. Doorly and F.T. Smith, Initial-value problems for spot disturbances in incompressible or compressible boundary layers. *J. Engng. Math.* 26 (1992) 87–106.
30. F.T. Smith, Steady and unsteady 3-D interactive boundary layers. *Computers & Fluids* 20 (1991a) 243–268. (Also given as a presentation at the R.T. Davis Memorial Symp., Cincinnati, U.S.A. (1987).)
31. F.T. Smith, On nonlinear effects near the wing-tips of an evolving boundary-layer spot. *Phil. Trans. Roy. Soc.* A340 (1992) 131–165.
32. M. Gaster, The development of three-dimensional wave packets in a boundary layer. *J. Fluid Mech.* 32 (1968) 173–184.
33. F.T. Smith, D.J. Doorly and A.P. Rothmayer, On displacement thickness, wall-layer and mid-flow scales in turbulent boundary layers, and slugs of vorticity in pipes and channels. *Proc. R. Soc.* A428 (1990) 255–281.
34. F.T. Smith and O.R. Burggraf, On the development of large-sized short-scaled disturbances in boundary layers. *Proc. R. Soc.* A399 (1985) 25–55.
35. V.J. Peridier, F.T. Smith and J.D.A. Walker, Vortex-induced boundary-layer separation. Part 1. The unsteady limit problem $\mathrm{Re}\rightarrow\infty$. *J. Fluid Mech.* 232 (1991a) 99–131.
36. V.J. Peridier, F.T. Smith and J.D.A. Walker, Vortex-induced boundary-layer separation. Part 2. Unsteady interacting boundary layer theory. *J. Fluid Mech.* 232 (1991b) 132–165.
37. F.T. Smith, Finite-time break-up can occur in any unsteady interacting boundary layer. *Mathematika* 35 (1988) 256–273.
38. F.T. Smith, Theoretical Aspects of Transition and Turbulence in Boundary Layers, *AIAA* paper no. 91-0331. (Also *AIAA J.* (1993). In the press.)
39. B.T. Dodia, R.G.A. Bowles and F.T. Smith, in preparation (1993).
40. R.G.A. Bowles, B.T. Dodia and F.T. Smith, in preparation (1993).
41. L.L. van Dommelen, Unsteady boundary-layer separation. *Ph.D. Thesis*, Univ. of Cornell (1981).
42. J.W. Elliott, S.J. Cowley and F.T. Smith, Breakdown of Boundary Layers: (i) on Moving Surfaces; (ii) in Semi-similar Unsteady Flow; (iii) in Fully Unsteady Flow. *Geophys. Astrophys. Fluid Dyn.* 25 (1983) 77–138.
43. S.J. Cowley, L.L. van Dommelen and S.T. Lam, On the use of Lagrangian variables in descriptions of unsteady boundary-layer separation. *Phil. Trans. Roy. Soc.* A333 (1991) 343–378.
44. S.N. Brown, H.K. Cheng and F.T. Smith, Nonlinear instability and break-up of separated flow, *J. Fluid Mech.* 193 (1988) 191–216.
45. K. Cassel, F.T. Smith and J.D.A. Walker, in preparation (1993).
46. J.M. Hoyle, Extensions to the theory of finite-time breakdown of unsteady interactive boundary layers. *Ph.D. Thesis*, Univ. of London (1991).
47. J.M. Hoyle and F.T. Smith, in preparation (1993).
48. F.T. Smith and R.I. Bowles, Transition theory and experimental comparisons on (I) amplification into streets and (II) a strongly nonlinear break-up criterion. *Proc. Roy. Soc.* A439 (1992) 163–175.
49. M. Nishioka, M. Asai and S. Iida, An experimental investigation of the secondary instability. in *Laminar-Turb. Transition*, Springer-Verlag (1979).
50. A.J. Grass, R.J. Stuart and M. Mansour-Tehrani, Vortical structures and coherent motion in turbulent flow over smooth and rough boundaries. *Phil. Trans. Roy. Soc.* A336 (1991) 35–65.
51. Y.S. Kachanov, O.S. Ryzhov and F.T. Smith, Formation of solitons in transitional boundary layers: theory and experiment. *J. Fluid Mech.* in press (1993).
52. B.T. Dodia, *Ph.D. Thesis*. Univ. of London (1994) in preparation.
53. P.A. Stewart and F.T. Smith, Three-dimensional nonlinear blow-up from a nearly planar initial disturbance, in boundary-layer transition: theory and experimental comparisons. *J. Fluid Mech.* 244 (1992) 79–100.
54. P.S. Klebanoff and K.D. Tidstrom, The evolution of amplified waves leading to transition in a boundary layer with zero pressure gradient. *Tech. Notes* Nat. Aero, Space Admin., Wash., D-195 (1959) (see in J.T. Stuart, ch. IX of *Laminar Boundary Layers*, ed. L. Rosenhead (1963)).